Title : will be set by the publisher
Editors : will be set by the publisher
EAS Publications Series, Vol. ?, 2002

AN INTRODUCTION TO VISIBILITY MODELING

Jean-Philippe Berger[1]

Abstract. This chapter is a first step towards visibility modeling. It describes analytical expressions for visibility curves derived from "classical" brightness distributions. It describes first some general useful tools for this kind of computation and then discusses several widely used morphologies. Finally, some practical issues of visibility modeling are discussed,

1 Introduction

Today, images are routinely produced by radio-interferometers such as the VLA or IRAM. Yet, this is not the case in the optical domain (infrared-visible wavelengths) where image reconstruction from a long baseline interferometer is still a celebrated achievement. Although visible/infrared interferometers have made enormous progress and will sooner or later lead to routine imaging, astronomers should be prepared to deal with visibility curves rather than true images. This should not prevent them from carrying out excellent scientific observations.

The purpose of this paper is to get the reader familiar with interpreting visibility data by describing visibility signatures of the most common morphologies. In Section 2 general tools for visibility computation are given. In Section 3 the most widely used morphologies are introduced; they are the "building blocks" of modeling. Finally in Section 4 we describe a few common issues that one might face in the process of interpreting visibility data.

It is beyond the scope of this paper to describe all the mathematical derivations, most of which are straightforward. Model fitting, which deserves further development, is only touched upon towards the end.

[1] Harvard Smithsonian Center for Astrophysics.
Cambridge, Ma, 02138 USA

DOI: (will be inserted later)

2 Computing visibilities: a general approach

2.1 Assumptions

The van Cittert- Zernike theorem (see C. Haniff, same volume) expresses the link between brightness distribution I of the object and the corresponding complex visibility ν. It is a Fourier transform.

$$I(\alpha,\beta) = \int_{-\infty}^{\infty}\int_{-\infty}^{\infty} \nu(u,v)\exp(2\pi i(\alpha u+\beta u))dudv \tag{2.1}$$

where (α,β) represents angular coordinates on the sky (units of radians) and (u,v) are the coordinates describing the baseline, and therefore the spatial frequencies of the brightness distribution. We can relate u and v to the baseline vector $\vec{B}$: $u = B_u/\lambda, v = B_v/\lambda$ where λ is the wavelength and B_u and B_v are the projection of the baseline vector on the two axes. Units for u and v are often expressed in fringe cycles per radian. The left part of Figure 1 illustrates these choices. Let us call $\vec{s}$ the vector arising from the center of the baseline and pointing towards the source; this defines the origin of the object coordinates. The reader interested in the orientation conventions should read D. Segransan's contribution in this volume.

The following discussions will be restricted to the pure monochromatic case. Reconstructing the brightness distribution from the complex visibilities is often not as simple as inverting visibility in Equation 2.1; a sampling function $S(u,v)$ that expresses the sparse (u,v) coverage has to be introduced as a multiplicating factor. The Fourier inversion no longer leads to the true brightness distribution but rather to the brightness distribution convolved with the "dirty" beam. Further numerical deconvolutions are required. Here we will restrict ourselves to the perfect and impossible case of continuous sampling, were the relation between visibility and brightness distribution is a pure Fourier transform.

Lastly, the complex visibility $\nu(u,v)$ is not normalized. It contains a scaling factor that is directly proportional to the intensity of the source. Here we will restrict the discussion to the normalized visibility V:

$$V(u,v) = \frac{\nu(u,v)}{\nu(0,0)} \tag{2.2}$$

One should keep in mind that the squared visibility is often the actual quantity measured by interferometers. For discussions involving flux integration and visibility modeling the reader is referred to an interesting actual application on young stars in Millan-Gabet *et al.* 2001.

2.2 Fourier transform

It is useful, before starting, to recall some basic properties of the Fourier transform which link brightness distribution and complex visibility.

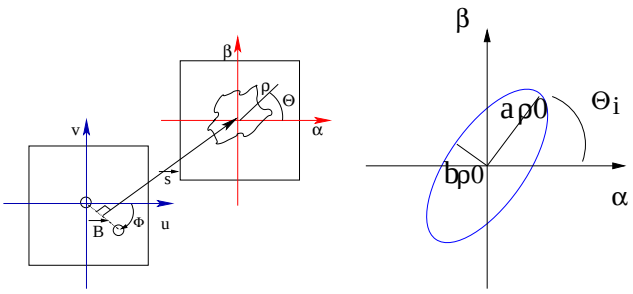

Fig. 1. Left: notations used in this chapter to describe the interferometer plane and the object brightness distribution plane. Right: ellipse in the object plane. $a\rho_0$ and $b\rho_0$ are semi-major and semi-minor axis and Θ_i the inclination with respect to the α axis.

$$\text{Addition :} \quad \mathrm{FT}\{I_1(\alpha,\beta)+I_2(\alpha,\beta)\} = \nu_1(u,v)+\nu_2(u,v) \tag{2.3}$$

$$\text{Similarity :} \quad \mathrm{FT}\{I(a\alpha,b\beta)\} = \frac{1}{|ab|}\nu(u/a,v/b) \tag{2.4}$$

$$\text{Translation :} \quad \mathrm{FT}\{I(\alpha-\alpha_0,\beta-\beta_0)\} = \nu(u,v)\exp[2\pi i(u\alpha_0+v\beta_0)] \tag{2.5}$$

$$\text{Convolution :} \quad \mathrm{FT}\{I_1(\alpha,\beta)\times I_2(\alpha,\beta)\} = \nu_1(u,v).\nu_2(u,v) \tag{2.6}$$

2.3 *Visibility curve for a circularly symmetric object.*

When the object has circular symmetry it is easier to switch to polar coordinates. The object brightness distribution being even and real, the corresponding visibility will consequently be even. We define $\rho=\sqrt{\alpha^2+\beta^2}$ and $\Theta=\mathrm{atan}\frac{\beta}{\alpha}$ as the polar coordinates in the object plane. We define $r=\sqrt{u^2+v^2}, \phi=\mathrm{atan}\frac{v}{u}$ are the polar coordinates in the (u,v) plane.

The expression for the visibility in polar coordinates can be extracted directly from the inversion of relation inverse of Equation 2.1, it is:

$$\nu(r,\phi)=\int_0^{2\pi}\int_0^{\infty} I(\rho,\Theta)\exp(-2\pi i(\rho r\cos(\Theta-\phi)))\rho d\rho d\Theta \tag{2.7}$$

Because of the symmetry $I(\rho,\Theta)=I(\rho)$ and $\nu(r,\phi)=\nu(\rho)$. Simplifying the cosine expression the previous equation becomes:

$$\nu(r)=\int_0^{2\pi}\int_0^{\infty} I(\rho)\exp(-2\pi i\rho r\cos\Theta)\rho d\rho d\Theta \tag{2.8}$$

Introducing the zeroth-order Bessel function of the first kind allows the computation of the integral with respect to Θ:

$$J_0(x) = \frac{1}{2\pi} \int_0^{2\pi} \exp(-ixcos\Theta) d\Theta \tag{2.9}$$

which leads to the final expression for the visibility:

$$\nu(r) = 2\pi \int_0^{\infty} I(\rho) J_0(2\pi\rho r) \rho d\rho \tag{2.10}$$

The link between ν and I is now a Hankel transform. This expressions allows us to compute visibility curves for a wide variety of distributions using the many relations linking Bessel functions (recurrence relations, distribution expressions etc...)

Another way of looking at Equation 2.10 is to consider the brightness distribution of a circular ring of infinitesimally thickness (radius ρ_0), which can be represented by the following brightness:

$$I(\rho) = \frac{1}{2\pi\rho_0} \delta(\rho - \rho_0) \tag{2.11}$$

the corresponding normalized visibility is then:

$$V(u,v) = J_0(2\pi\rho_0 r) \tag{2.12}$$

Any circularly symmetric function can be described as a sum (integral) of such rings with varying radius and intensities and therefore its Fourier transform logically corresponds to a sum (integral) of the corresponding visibility curves. This is of particular interest when one is dealing with the output of radiative transfer derivation or computation of circularly symmetric environments.

2.4 Inclined structure.

It is often the case that inclination is one of the unknown parameters when modeling an object. How to deal with an inclined circularly symmetric object ? We start by considering a circle projected at an inclination i on the plane of the sky then inclined with an angle Θ_i with respect to the orientation axes[1] (see right side of Figure 1). The circle is now an ellipse ring. Let us denote a and b respectively the semi-major axis and the semi-minor axis. The relation between a and b can be written as $b = a \cos i$. Estimating the visibility of such an object just requires a

[1] Remember that our choice of angle conventions is arbitrary although self-consistent.

change in the variables that will bring back the symmetry and therefore allows us to compute a Hankel transform. In our case the correct change in variable requires first a rotation of coordinate axes:

$$\begin{cases} u' &= u\cos\Theta_i + v\sin\Theta_i \\ v' &= -u\sin\Theta_i + v\cos\Theta_i \end{cases} \tag{2.13}$$

The equation of the ellipse ring then simply becomes:

$$\begin{cases} I(\alpha,\beta) &= \delta(\alpha,\beta) \\ \frac{\alpha^2}{a^2} + \frac{\beta^2}{b^2} = 1 \end{cases} \tag{2.14}$$

and a scaling in the object plane coordinates (similarity property):

$$\begin{cases} \alpha' = \frac{\alpha}{a} \\ \beta' = \frac{\beta}{b} \end{cases} \tag{2.15}$$

The ellipse ring is now a circle in the new (α',β') plane $(\alpha'^2 + \beta'^2 = 1)$. The visibility expression can be computed with a Hankel transform similar to equation 2.10 where $r = \sqrt{a^2u^2 + b^2v^2}$. The visibility of the ellipse ring is therefore:

$$V(u,v) = J_0(2\pi\rho_0\sqrt{a^2u^2 + b^2v^2}) \tag{2.16}$$

This can be directly applied to any elliptically symmetric brightness distribution.

2.5 A multicomponent object.

Let us consider now an astrophysical object that can be described by the addition of n components of known morphologies. Let us denote the brightness distributions of such objects $I_j(\alpha,\beta)$ their position in the plane of sky being (α_j,β_j) respectively and the corresponding normalized visibilities $V(u,v)$ with $j = 1..n$. To compute the normalized visibility of such an object one should take into account their respective contributions to the total brightness, which we will name F_j. The total brightness distribution can therefore be written:

$$I(\alpha,\beta) = \sum_{j=1..n} I_j(\alpha,\beta)\delta(\alpha-\alpha_j,\beta-\beta_j) \tag{2.17}$$

The addition property of the Fourier transform allows to write the visibility function as:

$$\nu(u,v) = \sum_{j=1..n} F_j V(u,v) \exp(2\pi i(u\alpha_j + v\beta_j)) \tag{2.18}$$

Normalization gives the final visibility:

$$V(u,v) = \frac{\sum_{j=1..n} F_j V(u,v) \exp(2\pi i(u\alpha_j + v\beta_j))}{\sum_{j=1..n} F_j} \tag{2.19}$$

We will make use of this expression in the next Section.

3 Common brightness distributions

3.1 The point source

A star sufficiently distant to be considered as a point source can be described by a Dirac distribution. Let us denote its coordinates with respect to the pointing center to be (α_0, β_0). The brightness distribution is then:

$$I(\alpha,\beta) = \delta(\alpha - \alpha_0, \beta - \beta_0) \tag{3.1}$$

Using the translation property of the Fourier transform it is then straightforward to demonstrate that the visibility is

$$V(u,v) = \exp^{-2\pi i(u\alpha_0 + v\beta_0)} \tag{3.2}$$

The amplitude of the visibility will be one, independently of the baseline. The phase is linearly dependent on the baseline. In the particular case were the star is at the pointing center the phase will be zero. From a practical point of view and in the absence of true phase reference (due to atmosphere, optomechanical instabilities etc.), the true phase is not measurable. The interest of observing a point source, i.e a star with a sufficiently small angular diameter, is that the measured visibility will allow access to the point spread function or in our context the instrumental visibility function.

3.2 The Gaussian disk

The Gaussian disk brightness distribution owes its success to its easy-to-compute Fourier transform. It is often used to estimate the size of a resolved envelope. The brightness distribution of a Gaussian with θ as full width to half maximum (FWHM) is:

$$I(\alpha,\beta) = \frac{1}{\sqrt{\pi/4\ln 2}\theta} \exp(\frac{-4\ln 2\rho^2}{\theta^2}) \tag{3.3}$$

where $\rho = \sqrt{\alpha^2 + \beta^2}$, and the corresponding visibility function is:

$$V(u,v) = \exp(-\frac{(\pi\theta\sqrt{u^2+v^2})^2}{4\ln 2}) \tag{3.4}$$

3.3 The uniform disk

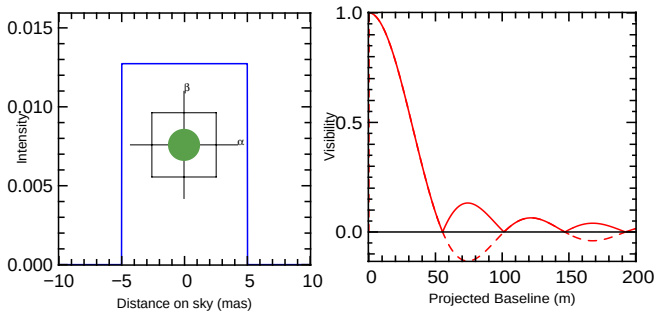

Fig. 2. Left: uniform disk model brightness distribution ($\theta = 10$mas). The curve represents a cut across the brightness distribution. Right: Corresponding visibility curve as a function of baseline ($\lambda = 2.2\mu$m). The solid line is the visibility amplitude the dashed line the complex one. Four zeros and five lobes are visible. The sign inversion in the complex visibility curve implies a 180° phase shift.

The uniform disk is the most simple model to describe the photospheric emission of a star (see Figure 2).

The brightness distribution of a disk of angular diameter θ is:

$$I(\rho) = \begin{cases} 4/(\pi\theta^2) & if\ \rho \leq \theta/2 \\ 0 & if\ \rho > \theta/2 \end{cases} \tag{3.5}$$

The corresponding complex visibility function, using Equation 2.10 is:

$$V(u,v) = 2\frac{J_1(\pi\theta r)}{\pi\theta r} \tag{3.6}$$

where r represents the radius in the (u,v) plane (or the projected baseline in number of wavelengths units) and J_1 is a first-order Bessel function of the first kind.

This is the first model to use when one wants to extract a diameter from a visibility curve. The visibility curve has several zeroes whose positions can be directly related with the diameter. If B_1 is the baseline corresponding to the first zero, then the diameter in milliarcseconds is $\theta = 251.6''\lambda/B_1$. Finding the

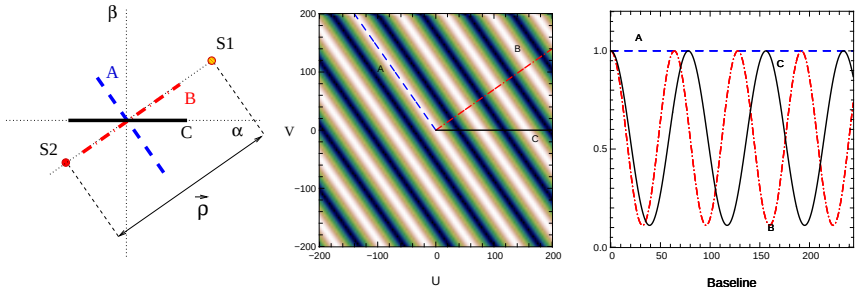

Fig. 3. Left: an unequal binary the plane of the sky. The binary separation ρ is 5 mas, the PA $\theta = 35°$, the flux ratio 0.5, and the wavelength of observation 1.55μm. The lines symbolizes three different baselines with different projected angles (dashed (A): 125°, dash-dotted (B): 35°, solid (C): 0°). Center: Image of the square of the visibility amplitude in the (u,v) plane obtained for such a binary. The lines show what part of the (u,v) is explored with the previous baselines. A maximum baseline of 200 m has been choosen here. Right: Corresponding square visibility curves corresponding to the three baselines (see text for comments).

first zero is of course not mandatory, a χ^2 minimization on a properly sampled visibililty curve is the best way to get an accurate final result.

Note that Equation 3.6 shows that visibility changes sign as it goes through the zero. The observational consequence of this is that the interferogram phase shifts by 180°. Because phase is lost in the measurement process, this won't be directly observable but can be recovered by the measurement of closure phases (see J.D. Monnier same volume).

Any departure from the uniform disk model, caused for example by limb-darkening or brightening or the presence of a hot spot, should mostly affect spatial frequencies higher than the first null and therefore should require exploration of the second lobe. The reader is referred to the work by J. Young (same volume) for more details.

3.4 The binary

Binary star observations, together with diameter measurements, are the most widespread scientific observations made with interferometers so far. We can now use the same procedure as described in Section 2.5 to compute the visibility. The expression of the brightness distribution of a binary system (stars S_1 and S_2) with separation ρ, position angle θ and respective fluxes F_1 and F_2 is simply the sum of two unresolved point brightnesses (see Figure 3 and Equation 3.1).

$$I(\alpha,\beta) = F_1\delta(\alpha-\alpha_1,\beta-\beta_1) + F_2\delta(\alpha-\alpha_2,\beta-\beta_2) \tag{3.7}$$

where (α_1, β_1) and (α_2, β_2) are the angular coordinates for stars S_1 and S_2. The corresponding Fourier transform gives the unnormalized complex visibility function:

$$\nu(u,v) = F_1 \exp(2\pi i(u\alpha_1 + v\beta_1)) + F_2 \exp(2\pi i(u\alpha_2 + v\beta_2)) \tag{3.8}$$

The normalized squared visibility amplitude is then:

$$|V(u,v)|^2 = \frac{\nu(u,v)\nu(u,v)^*}{|\nu(0,0)|^2} \tag{3.9}$$

$$= \frac{F_1^2 + F_2^2 + 2F_1F_2\cos(2\pi(u(\alpha_1 - \alpha_2) + v(\beta_1 - \beta_2)))}{(F_1 + F_2)^2} \tag{3.10}$$

where the normalisation factor is the total flux squared $(\nu^2(0,0))$. If we introduce the flux ratio $f = \frac{F_2}{F_1}$ the baseline vector $\vec{B}$ ($|B| = \lambda\sqrt{u^2 + v^2}$) and the separation vector $\vec{\rho}$ ($|\rho| = \sqrt{(\alpha_1 - \alpha_2)^2 + (\beta_1 - \beta_2)^2}$) Equation 3.10 becomes:

$$|V(u,v)|^2 \quad = \quad \frac{1 + f^2 + 2f\cos(2\pi/\lambda\vec{B}\vec{\rho})}{(1+f)^2} \tag{3.11}$$

Figure 3 shows a binary example ($|\vec{\rho}|$= 5 mas, the PA 35° and f=0.5). The corresponding squared visibility in the (u,v) plane is displayed in the center. It has a typical rippled structure. When looking at a squared visibility curve along three different projected baselines (at right in Figure 3) one can see very different responses [2]. Projected baseline A is perpendicular to the line linking the two components. Consider the analogy to the Young's Double Slit Experiment with two sources instead of one. If the projection of the line between the two sources along the optical axis [3] is perpendicular to the line between the two holes, then the optical path from one source to each of the two slits is the same. Therefore the fringe center for the two sources will be located at the same point in the screen whatever the distance between the slits. No visibility variation with slit separation is to be expected.

Two other baselines at two different angles will lead to two curves with different periods but the same amplitude. However it is most probable in practice that the earth rotation will lead to non linear cuts accross the (u,v) plane.

Now let us consider that both stars have finite size, i.e can be resolved by the interferometer. If $V_1(u,v)$ and $V_2(u,v)$ are the visibility curves for S_1 and S_2 stars respectively it is easy to write the expression of the visibility for the binary:

[2] These baseline coverages are of course unrealistic since earth rotation will induce elliptical tracks in the (u,v) plane

[3] The optical and pointing axis is defined for example as the line linking the center of the two sources to the center of the two slits.

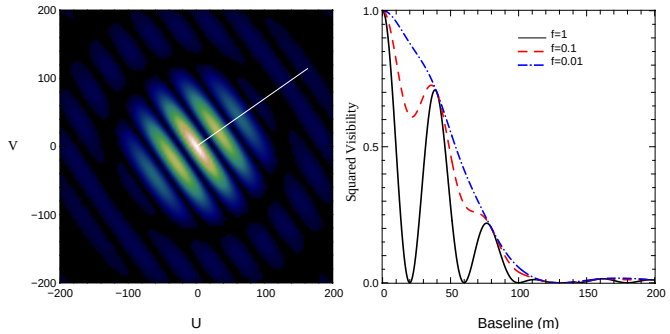

Fig. 4. Left: squared visibility in the (u, v) plane for a binary whose two stars have uniform disk diameters of 3 mas and are separated from each other by 8 mas (realistic ?) with a position angle 35° ($\lambda = 1.55\mu$m). The left side of the figure displays the squared visibility expected in the (u, v) plane when the flux ratio is one. The right side shows the squared visibility curves as a function of baseline (oriented at PA 35°) for three different flux ratios (solid, dash, dashdot curves respectively correspond to $f = 1, 0.1, 0.01$.

$$V(u,v) = \frac{V_1^2 + f^2 V_2^2 + 2f|V_1||V_2|\cos(2\pi/\lambda \vec{B}\vec{\rho})}{(1+f)^2} \tag{3.12}$$

Figure 4 shows the squared visibility as a function of baseline for a binary whose two stars are also resolved. The squared visibility curves appear as a modulation of the classical uniform disk shape by a cosine function caused by the binary. The amplitude of the modulation decreases when the flux ratio gets smaller. For a flux ratio of $f = 0.001$ the influence of the companion is barely noticeable.

In fact, Equation 3.12 can be used for any kind of structure involving two different components for which individual visibilities are known, for example a star+ envelope system.

4 Common issues.

Before and after preparing observations the astronomer will have to make use of visibility models. Before because a minimum a priori knowledge about what the object could be is mandatory to make the right choices of baselines configurations and instrument parameters. After to try to fit the visibility data obtained in order to constrain model parameters. We discuss here some common issues the astronomer will encounter in that context.

4.1 How to choose the optimal (u,v) coverage ?

When preparing an actual observation with the VLTI the astronomer will have to choose between several possible telescope array configurations. Many questions

will probably arise. Here are two very common ones.

What if the object contains multiple components ?

The influence of one of the components in an astrophysical multi-component objet depends on its size but also on its relative contribution to the total brightness. Let us take for example a star+disk model and two extremes cases - the disk is extended but faint with respect to the star and the disk is small but bright. These objects can lead to the same visibility measurements at sufficiently long baselines. The contrast between the different components of the object (sizes and brightnesses) translates into a constraint in the choice of (u, v) positions to sample each object with sufficient spatial frequency coverage but also to a constrain in the visibility accuracy. This latter constrain is directly related with the dynamic range accessible. As another example we can look back at figure 4. In that case the astronomer has to be prepared to sample enough (u, v) plane to see the envelope and the modulation which do not appear at the same scales. He has also to worry about dynamic range, -detecting a flux ratio of 0.01 requires accurate visibilities.

Where should we sample the (u, v) *plane ?*

Let us take the example of the uniform disk model. We can convince ourselves by plotting the first derivative of the Bessel function that the closer to the minimum the measurement is made, the more constraining it will be. However, the smaller the visibility will be the smaller the signal to noise ratio. We can see that, in the photon starving regime, there is a compromise to be found between high-visibility (therefore high signal to noise ratio (snr)) and poor constraints on the curve, and low visibililty (low snr) but higher constraint. A good thing to do for preparing any kind of observation is to plot the first derivative of the expected visibility function with respect to the parameters as a function of baseline. This will reveal the positions in the (u, v) plane which would most constrain the parameters.

4.2 Superresolution and its limitations.

If the object's angular size is too small to be resolved in the classical sense (object bigger than the beam size as defined by the length of the projected baseline) it is still possible to derive quantitative parameters from its visibility curve (superresolution). This is because modeling visibilities is a deconvolution process. However, one should remember that if components are barely resolved it will be hard to find out which is the best choice of model, since all the basic visibilities described earlier have quadratic dependencies toward small spatial frequencies. The definition of "barely resolved" will of course depend on the accuracy with which the visibility measurements are made.

Figure 5, extracted from Millan-Gabet *et al.* (1999) is an illustration of that topic. It shows the visibility measurements made on the Herbig AeBe star AB Aurigae with the IOTA and PTI interferometers. One can clearly see that the combination of limited visibility accuracy and a lack of points towards the longest baselines precludes from characterizing the emitting structure. A gaussian envelope, uniform disk and ring can be successfully used to fit the visibility points.

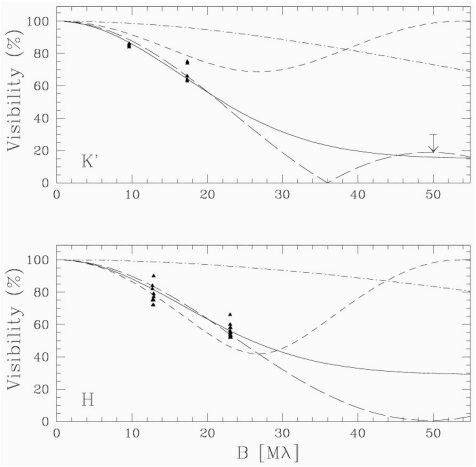

Fig. 5. Model fitting of visibilities measured with the IOTA and PTI interferometers on the Herbig star AB Aurigae (Millan-Gabet *et al.* 1999). Top of figure corresponds to the K' band, bottom to the H band. IOTA points are the filled triangles and the PTI measurement provides an upper limit at long baseline. The absence of measurements at long baselines prevents us from constraining the morphology of the emitting region. Short dash-binary, solid line-gaussian envelope, long dash-resolved ring and dash dotted line-accretion disk model. Gaussian and ring model are indistinguishable at the shortest baselines.

4.3 Model fitting.

The number of physical parameters describing the observed object will obviously depend on the number of independent visibility points at different locations in the (u, v) plane. Choosing the right number of parameters is not always an easy task. The whole fitting process requires several steps which can be very crudely summarized by:

1. choosing the model and its parameters.
2. defining a likelihood function linking visibility and their errors and the parameters of the model.
3. using the maximum likelihood method, i.e. minimizing a χ^2 to constrain the parameters.

In practice several problems can arise. Among them finding the correct χ^2 to minimize (it is not always correct to use a least square fitting method) or finding local minima leading to inexact parameters. It is always a good idea to start the model fitting process by an inspection of the date and some ad hoc attemps to reproduce the visiblity features with the most common models. This provides

a first estimation of the parameter ranges and may guide the fitting process to appropriate regions that avoid local minima.

References

Millan-Gabet, R. *et al.* 2001, ApJ, 546, 358
Millan-Gabet, R. *et al.* 1999, ApJ, 513,L131